https://doi.org/10.5194/egusphere-2025-5893
Preprint. Discussion started: 4 December 2025

Changes in the frequency and intensity of concurrent extreme wind speed and precipitation days over China during 1981–2022

Kangmin Wen[1, 2], Jun Shi [3]

[1]Fujian Institute of Meteorological Sciences, Fujian Meteorological Bureau, Fuzhou, 350028, China
[2]Fuzhou Intelligent Meteorological Industry Technology Innovation Center, Fuzhou Meteorological Bureau, Fuzhou, 350028, China
[3]Shanghai Ecological Forecasting and Remote Sensing Center, Shanghai Meteorological Bureau, Shanghai, 200030, China

Correspondence to: Jun Shi (sunrainlucky@qq.com)

Abstract. Compound extreme wind speed and extreme precipitation days (CWPDs) can significantly impact production and living, socio-economies, and human health. However, most previous studies have used fixed percentile thresholds to determine wind speed and precipitation extremes. This study investigated the characteristics and dynamics of CWPDs during 1981–2022 in mainland China based on the time-varying daily thresholds by using daily maximum wind speed and precipitation observation data. The results indicated that CWPDs were most likely to occur in southeastern South China (SC), Hainan Province, the northwestern parts of the middle and lower reaches of Yangtze River (YR), some scattered areas in the central and eastern YR. Annual CWPDs decreased in mainland China during 1981–2010, and then showed an obvious upward trend after 2010. Different percentile thresholds had effects on the spatial pattern and change trend of CWPDs. Spatially, CWPDs decreased more in parts of eastern Southwest China (SWC), YR, southeastern North China (NC) and central Northeast China (NEC), but less in mid-northern NC and most of Northwest China (NWC). In most areas of mainland China, the CWPDs frequencies under the four thresholds all showed decreasing trends, as the threshold increased, the trends of decreased for CWPDs frequencies decreased. With the increase of the threshold, the range of CWPDs with stronger intensity further reduced. CWPDs intensities were more severe in eastern coastal areas of YR, mid-eastern SC, parts of eastern SWC, parts of central NEC, parts of northwestern NWC and mid-northern in Hainan Province. Annual CWPDs intensities changed obvious around early-to-mid 2010s in under four different thresholds. With the increase of the threshold, the weakening trends of annual CWPDs intensities further weakened and even slightly strengthened during 1981-2022. The CWPDs intensities under the four thresholds all showed decreasing trends in most areas of mainland

https://doi.org/10.5194/egusphere-2025-5893
Preprint. Discussion started: 4 December 2025

China except for parts of central SC, a few scattered areas of YR, several scattered areas of NC and NEC, a few scattered areas of NWC, individual areas of eastern SWC. As the thresholds increased, the trends of weakened for CWPDs intensities decreased and the scopes with a slight strengthening trend expanded. The changes of extreme wind speed days were consistent with those of CWPDs during 1981–2010 and 2011–2022, but the changes of extreme precipitation days and CWPDs were not corresponding. Due to the increase of extreme wind speed days and the accelerated increase of extreme precipitation days after 2010, the CWPDs changed from decrease before 2010 to increase after then. We conclude that the annual cumulative value obtained through time-varying thresholds and the latest daily observations can yield new insights into compound extremes.

Key words. Concurrent, extreme wind speed days, extreme precipitation days, characteristics, trends, China

https://doi.org/10.5194/egusphere-2025-5893
Preprint. Discussion started: 4 December 2025

1 Introduction

The increase in the frequency and intensity of weather and climate extremes (e.g. drought, flood, heat wave, cold wave) has been shown to be associated with global warming (Stocker et al., 2013; Naumann et al., 2018; Trenberth et al., 2014), which can pose huge risks to socio-economic and natural biophysical systems. Compound extremes are triggered by the simultaneous appearance of multiple climate disasters or drivers and may generate amplified impacts than individual extreme. Compound wind speed and precipitation extremes as the typical combined extreme events, induced flooding and strong winds can damage public transportation, cause power shortage, and destroy construction, which can also increase the vulnerability of the influenced areas to subsequent extremes, even moderate compound extremes (Chen et al., 2021; Yaddanapudi et al., 2022). Hence, Compound wind speed and precipitation extremes are the aspects that the insurance industry is very interested in, as the extremes can cause losses beyond the designed insurance coverage (e.g., Hamid et al., 2011). Compound extremes can occur by accident and be causally irrelevant, or they can be caused by the same underlying weather process or system (Seneviratne et al., 2012). Simultaneous precipitation and wind speed extremes are often relevant. In the areas of subtropics and midlatitudes, for instance, they can be related with strong extratropical cyclones (Liberato, 2014; Raveh-Rubin and Wernli, 2015). In the areas of subtropics and tropics, simultaneous precipitation and wind speed extremes can be triggered by tropical cyclones (Federal Emergency Management Agency, 2013; Rodgers et al., 1994). Thus, the analysis of the change characteristics of wind speed and precipitation-related extremes can provide a decision-making reference for rational planning and allocation of grain resources, maintaining regional stability, protecting the transportation and electricity, actively coping with the risks brought by future climate change, and reducing the impact of natural disasters on human life.

Some studies have devoted to spatio-temporal variation (Martius et al., 2016; Li et al., 2022), future projections (Yaddanapudi et al., 2022; Ridder et al., 2020, 2022; Zscheischler et al., 2021) or develop new methodology (Tilloy et al., 2022; Zscheischler et al., 2021) to evaluate the compound wind speed and precipitation extremes over various regions of the world. Other studies have investigated the mechanisms and impacts of compound extremes (Li et al., 2022; Waliser and Guan, 2017). Martius et al. (2016) made the first global quantification of compound precipitation and wind extremes, indicating that compound precipitation and wind extremes mainly happen in coastal regions those frequently affected by tropical cyclones (TCs). Zscheischler et al. (2021) analysed concurrent wind and precipitation extremes in different high-resolution simulations and reanalysis data for central Europe, and found the key factor in explaining differences in the dependence behavior between strong wind and heavy precipitation between simulations might be the boundary conditions in WRF, and offered new method to assess climate model simulations with respect to compound extremes. Li et al. (2022) showed that the areas that the most frequent, strongest, and longest-lasting affected by concurrent wind and precipitation extremes in summer in recent decades occur in northwestern Pacific Ocean and its coasts, which are caused by cyclones, and compare to increasing trends in equatorial tropical regions, the number of concurrent wind and precipitation extremes over southern China shows a significant downward trend. Yaddanapudi et al. (2022) indicated a remarkable rise in extreme

https://doi.org/10.5194/egusphere-2025-5893
Preprint. Discussion started: 4 December 2025

precipitation compared with individual extreme wind events under climate change. The likelihood of compound wind and precipitation extremes events under climate change shows an increase (about 40%–50%) in most coastal areas in East, and South Asia, and North Atlantic. Waliser and Guan (2017) discerned strong relation between individual extreme wind or extreme precipitation and atmospheric rivers (ARs) across broad swathes of midlatitudes from the perspective of univariate, indicated that of ARs as a potential driver of compound wind and precipitation extremes.

Although there have been some studies on the spatial and temporal characteristics and dynamics of compound wind speed and precipitation extremes, most of them are based on grid data, for instance, the Gridded data from the model simulations (Van den Hurk et al., 2015; Yaddanapudi et al., 2022; Zscheischler et al., 2021), or climate reanalysis data (Raveh-Rubin and Wernli, 2015; Martius et al., 2016; Ridder et al., 2020; Zscheischler et al., 2021), so the results are less accurate than ground-based observations. Meanwhile, some studies have focused only on a single season (Li et al., 2022; Zscheischler et al., 2021), in fact, hot and dry conditions can also occur in all seasons. In addition, most of the previous studies have calculated the compound extremes according to the stable relative percentile thresholds, and the analysis of the compound wind speed and precipitation extremes base on the time-varying thresholds is lacking.

Therefore, the objective of this study is to investigate the changes in the spatial and temporal characteristics of compound extreme wind speed and extreme precipitation days (CWPDs) over mainland China base on the time-varying thresholds using the ground observation data of daily time scale. The time-varying thresholds of extreme wind speed day and extreme precipitation day at each station were first calculated. The spatial and temporal characteristics and changes of CWPDs over mainland China were then assessed, and finally, the results were discussed and compared and a summary of the main conclusions was provided.

2 Data and methods

2.1 Data

Two long-term daily historical observation datasets of daily maximum wind speed and daily total precipitation from 1686 meteorological stations over mainland China were used. These datasets were from the National Meteorological Information Center of the China Meteorological Administration (NMIC/CMA) (http://data.cma.cn/). The data had undergone strict quality control before release and had been widely applied in related research (Li et al., 2015; Yu and Zhai, 2020). To ensure the consistency and integrity of the daily sequences, if the percentage of missing daily records at a station exceeded 20% of the total daily records from 1981 to 2022, the meteorological station would be removed from the dataset of this study. Ultimately, 1686 meteorological stations were selected for analysis (Fig.1). Among the 1686 stations, there were 1292 stations with the missing rate of daily maximum wind speed records of less than 3%, and 1654 stations with that of daily precipitation records of less than 3% during 1981–2022. The missing records of wind speed and precipitation in any station were retained.

https://doi.org/10.5194/egusphere-2025-5893
Preprint. Discussion started: 4 December 2025

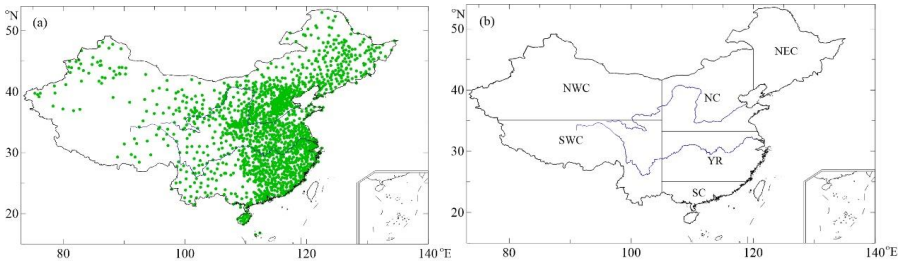

Figure 1. The locations of 1686 meteorological stations (a) and the boundaries of the divided six regions (b). NEC, NC, NWC, SWC, YR and SC represent Northeast China, North China, Northwest China, Southwest China, the middle and lower reaches of Yangtze River and South China, respectively, the same as below.

2.2 Definition of compound extremes

CWPDs were defined as simultaneous occurrence of extreme wind speed day and extreme precipitation day on the same day at a given station. Since there are significant differences in wind speed and precipitation among different seasons in China, it is obviously inappropriate to choose a fixed threshold for extreme wind speed and extreme precipitation to analyze the climate changes caused by extreme wind speed and extreme precipitation. Therefore, we use the time-varying threshold to define extreme wind speed and extreme precipitation. When the weather state deviates significantly from its climate average state, it is considered an event that is unlikely to occur, that is, an extreme event. Similarly, because the wind speed and precipitation vary greatly in different parts of China, it is obviously inappropriate to use the same fixed extreme wind speed threshold and extreme precipitation threshold for all stations across the country to analyze climate change caused by extreme wind speed and extreme precipitation. Therefore, we used spatial change thresholds, that is, different extreme wind speed and extreme precipitation thresholds have been defined for different stations to analyze the climate change characteristics of local extreme wind speed and extreme precipitation.

The sliding average method was employed to determine the thresholds sequences (Wang et al., 2021). We use time-varying thresholds sequences to define extreme wind speed and extreme rainfall. The percentage on a daily basis is calculated from a 15-day time window centered on each calendar day (7 days before and after a given day) from 1981-2010 (i.e., total daily sample: 15 x 30 = 450 days). The time windows slide on a day-length basis, so the time windows overlap, connecting the end of one year to the beginning of the next, and when calculating the thresholds for the beginning of 1981 and the end of 2010, the data for 1979 and 2011 are used. Concurrent extreme wind speed and extreme precipitation days (CWPDs) were defined in this study as simultaneously meeting the conditions of extreme maximum wind speed and extreme rainfall for the same day at a given station. We separately used the 85^{th}, 90^{th}, 95^{th} and 98^{th} percentiles of daily maximum wind speed values during 1981–2010 as extreme wind speed thresholds, the 85^{th}, 90^{th}, 95^{th} and 98^{th} percentiles of daily precipitation values

https://doi.org/10.5194/egusphere-2025-5893
Preprint. Discussion started: 4 December 2025

during 1981–2010 as extreme precipitation thresholds. Percentiles were defined based on the non-zero values of daily maximum wind speed and precipitation from 1981 to 2010. One compound day defined when the daily maximum wind speed higher than the percentile and the daily precipitation amount higher than the percentile at the same time. Four combinations of wind speed and precipitation thresholds were used in this study, including 85th and 85th (W85∩P85), 90th and 90th (W90∩P90), 95th and 95th (W95∩P95), 98th and 98th (W98∩P98).

To measure the intensity of concurrent days, we established the CWPD index (CWPDI) as a combination of wind and precipitation extremes (Zhang et al., 2021). For each station, we applied a range normalization formula to normalize daily maximum wind speed ($RWND_i$) and precipitation ($RPCP_i$) during 1981–2022 to a range of 0–10, respectively.

$$R_i = \frac{x_i - x_{min}}{x_{max} - x_{min}} \cdot 10$$

where R_i and x_i are the ith range normalized result and input data, respectively. x_{max} and x_{min} are the maximum and minimum values of the input data series, respectively. For one CWPD (one day) at a given station, CWPDI can be calculated as follows:

$$CWPDI_i = RWND_i \cdot RPCP_i$$

where i is the time step (i =1, 2, 3, …, n) of a certain variable at each station; $RWND_i$ and $RPCP_i$ are respectively the ith normalized maximum wind speed and precipitation values that meet the CWPD criterion. For a given station, the annual CWPDI is the total CWPDI of all CWPDs within a year. For all stations of China at the same day, cumulative CWPDI summarizes the total CWPDI of CWPD at each station. We summed the CWPDI values of all stations in China on each day (1981–2022) to determine the daily cumulative CWPDI values in descending order, ultimately isolating the top 10 concurrent extremes for further analysis.

2.3 Regional division and linear trend

The meteorological observation stations in mainland China are dense in the eastern region but sparse in the western region. In order to eliminate the spatial sampling error in regional statistics, the means of grid area weighting (Jones and Hulme, 1996) was utilized when calculating the regional sequences of the concerned regions. This method separated the corresponding region into 2.5 ° × 2.5 ° longitude and latitude grids, and calculated the internal mean of each grid. The regional sequences were then obtained by weighting the latitude values of the center points of all grids.

To analyze the changing characteristics of CWPDs in different regions of China, with reference to the previous commonly used climate division methods (Xu et al., 2011; Shi et al., 2016), the mainland China was divided into six regions (Fig. 2), namely Northeast China (NEC), North China (NC), Northwest China (NWC), Southwest China (SWC), the middle and lower reaches of Yangtze River (YR) and South China (SC). The long-term linear trends of the concerned sequences were estimated by utilizing the Sen-Theil method (Sen, 1968; Theil, 1992), and the significance was tested via the Mann-Kendall method (Mann, 1945; Alizadeh et al., 2020). Mann-Kendall trend test is a

https://doi.org/10.5194/egusphere-2025-5893
Preprint. Discussion started: 4 December 2025

nonparametric test, which is widely applied to statistically evaluate whether a monotonic trend exists in the time sequences of the given variables. A linear trend was regarded statistically significant when it passed the significant test of the 95% confidence level ($p < 0.05$).

The changes in compound extremes are closely related to the trend changes of individual variables and the changes in the dependencies among variables (Zscheischler and Seneviratne 2017). The dependency relationship among variables directly affects the occurrence probability of compound extremes (R. Wang et al. 2021). To further explore the dependence of CWPDs on individual extreme wind speed or extreme precipitation days, considering the sample size and representativeness comprehensively, the threshold combination of W85∩P85 was selected, and the interannual and spatial patterns of the frequency ratios of CWPDs to extreme wind speed days and extreme precipitation days, as well as the spatial trends of the frequencies of CWPDs, extreme wind speed days, and extreme precipitation days were compared.

3 Results

3.1 Characteristics of CWPDs frequency at different thresholds

In mainland China, different percentile thresholds had certain effects on the spatial pattern of the frequency of CWPDs. In general, CWPDs were more frequent in southeastern SC, Hainan Province, northwestern YR, some scattered areas in the central and eastern YR, but less in most of NWC, SWC, NEC and NC (Fig. 2).

Under the threshold of W85∩P85, annual mean CWPDs were more in most SC and YR, Hainan Province, a small area in eastern SWC, a few area in southeastern NC, a small area in northern NWC and northern NEC from 1981 to 2022, with frequencies of 5-9 days, among which the most annual CWPDs were 9-13.4 days, occurred in mid-southern SC, a small number of stations in the western and mid-eastern YR, some individual stations in the eastern SWC and northern NWC (Fig. 2a). CWPDs were less in most NWC, SWC, NEC and NC, with values ranging from 0.4 to 5 days. Under the threshold of W90∩P90, the frequency distribution is similar to the threshold of W85∩P85, but the areas with higher frequencies have decreased. CWPDs were more in southeastern SC, Hainan Province, northwestern YR, some scattered areas in central and eastern YR, a small area in eastern SWC, a small area in northern NWC and northern NEC, with annual values ranging from 3 to 8.5 days (Fig. 2b). CWPDs were less in most NWC, SWC, NEC and NC, ranging from 0 to 3 days.

Under the threshold of W95∩P95, the frequency distribution is similar to the threshold of W90∩P90, but the areas with higher frequencies have further decreased. Annual mean CWPDs were more in southeastern SC, Hainan Province, northwestern YR, some scattered areas in central and eastern YR, a small area in eastern SWC, a small area in northern NWC and northern NEC, ranging from 1 to 3.6 days (Fig. 2c). CWPDs were less in most NWC, SWC, NEC and NC, with a range of 0 to 1 days. Under the threshold of W98∩P98, annual mean CWPDs were more in southern SC, Hainan Province, a small area in northwestern YR, a small area in the eastern coastal areas of YR, a small area

https://doi.org/10.5194/egusphere-2025-5893
Preprint. Discussion started: 4 December 2025

in eastern SWC, with annual values ranging from 0.4 to 1.36 days (Fig. 2d). CWPDs were less in most NWC, SWC, NEC, NC and YR, with a range of 0 to 0.4 days.

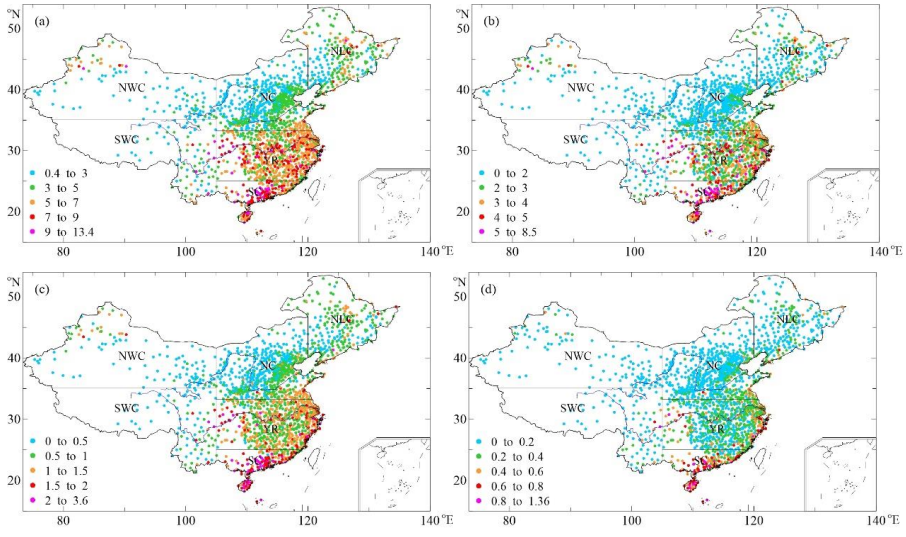

Figure 2. Annual average (Units: days per year) of CWPDs frequencies at different thresholds in mainland China during 1981–2022. (a: W85∩P85; b: W90∩P90; c: W95∩P95; d: W98∩P98)

Annual CWPDs decreased in mainland China during 1981–2010, and then increased more quickly, that is, CWPDs showed a more obvious upward trend after 2010 (Fig. 3). From 1981 to 2022, The CWPDs under the four thresholds of W85∩P85, W90∩P90, W95∩P95 and W98∩P98 decreased significantly at a rate of 0.54, 0.18, 0.10 and 0.02 days per decade, respectively, with the annual average of 4.08, 2.22, 0.74 and 0.20 days. With the heightening of the threshold, the decreasing trend of the frequency of CWPDs had slowed down.

In different periods, the change characteristics of CWPDs were different, and even in the same period, the change trend of CWPDs and its significance level were also related to the selection of threshold. During 1981–2010, annual CWPDs under the thresholds of W85∩P85, W90∩P90, W95∩P95 and W98∩P98 decreased at a rate of 0.96, 0.57, 0.22 and 0.07 days per decade, respectively (Fig. 3a-3d), and all the trends were statistically significant. During 2011–2022, CWPDs under the threshold of W85∩P85, W90∩P90, W95∩P95 and W98∩P98 increased significantly at a rate of 1.17, 1.92, 0.32 and 0.10 days per decade, respectively (Fig. 3a-3d).

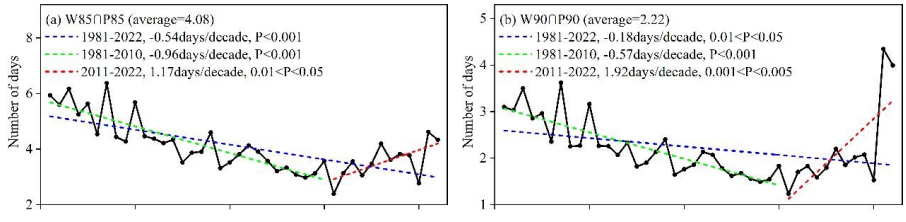

https://doi.org/10.5194/egusphere-2025-5893
Preprint. Discussion started: 4 December 2025

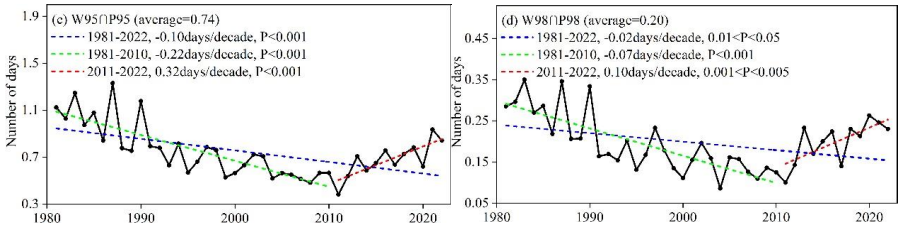

Figure 3. Inter-annual changes of CWPDs frequencies at different thresholds in mainland China during 1981–2022. The colored dashed lines are linear trends estimated by the Sen-Theil method, the same as below.

From 1981 to 2022, the CWPDs frequencies under the four thresholds all showed decreasing trends in most areas of mainland China, CWPDs decreased more in parts of eastern (Southwest China) SWC, YR, southeastern North China (NC) and central Northeast China (NEC), but less in mid-northern NC and most of Northwest China (NWC). In most areas of mainland China, as the threshold increased, the rates of decreased for CWPDs frequencies decreased (Fig. 4). Under the threshold of W85∩P85, the declining trends of 1-3.9 days per decade of CWPDs frequencies mainly occurred in most YR, most NEC and SWC, northwestern and southeastern NWC, parts of northern and southern NC**.** The CWPDs frequencies decreased at rates of 0-1 days per decade mainly occurred in central NWC, parts of central and southern NC, a little parts in mid-southern NEC. The rising trends more than 1 days per decade mainly including central NC, central SC, eastern of Hainan Province, a small area in eastern SWC, and a few scattered areas in YR (Fig. 4a). Under the threshold of W90∩P90, the spatial distribution of changing trends for CWPDs frequencies were similar to the threshold of W85∩P85, the decreasing trends of 0.7-2.7 days per decade of CWPDs frequencies mainly occurred in most YR, parts of NEC, parts of eastern SWC and southern NC, and parts of northwestern and southeastern NWC. The CWPDs frequencies decreased at rates of 0-0.7 days per decade mainly occurred in most NC, central NWC, parts of mid-southern NEC. The rising trends of 0.7-1.7 days per decade mainly occurred in a few scattered areas in mid-southern NC and northwestern YR. The increasing trends more than 1.7 days per decade mainly including central SC, eastern of Hainan Province, a few scattered areas in YR (Fig. 4b).

Under the threshold of W95∩P95, there weren't many obvious changes for the spatial pattern of changing trends of CWPDs frequencies compared with the threshold of W90∩P90, the reducing trends of 0.3-1.3 days per decade of CWPDs frequencies mainly occurred in most YR, parts of eastern SWC, northwestern NWC, western of Hainan Province, a few scattered areas in NEC. The CWPDs frequencies decreased at rates of 0-0.3 days per decade in most NC, parts of mid-eastern NWC, parts of eastern SC, and a few scattered areas in NEC. The increasing trends more than 0.8 days per decade including central SC, a few scattered areas in YR, some individual areas in eastern SWC and southern NC. The increasing trends between 0.3-0.8 days per decade including some individual areas in southern NC, some scattered individual areas in YR (Fig. 4c). Under the threshold of W98∩P98, the number of stations showing an increasing trend has significantly increased compared to the threshold of W90∩P90. The CWPDs frequencies decreased at rates of 0.1-0.5 days per decade in most YR, a little parts eastern SWC, parts of northwestern NWC, parts of southern NC and western SC, central of Hainan Province, a few scattered areas in NEC. The CWPDs frequencies decreased with trends of

https://doi.org/10.5194/egusphere-2025-5893
Preprint. Discussion started: 4 December 2025

0-0.1 days per decade showed in parts of central and southwestern NC, parts of mid-eastern NWC, and a few scattered areas in NEC. The increasing trends of 0.1-0.2 days per decade mainly including some individual areas in central NC, some scattered individual areas in YR. The rising rates more than 0.2 days per decade occurred in central SC, a few scattered areas in YR and mid-southern NC, some individual areas in eastern SWC, some individual areas in southern NEC and northern NEC (Fig. 4d).

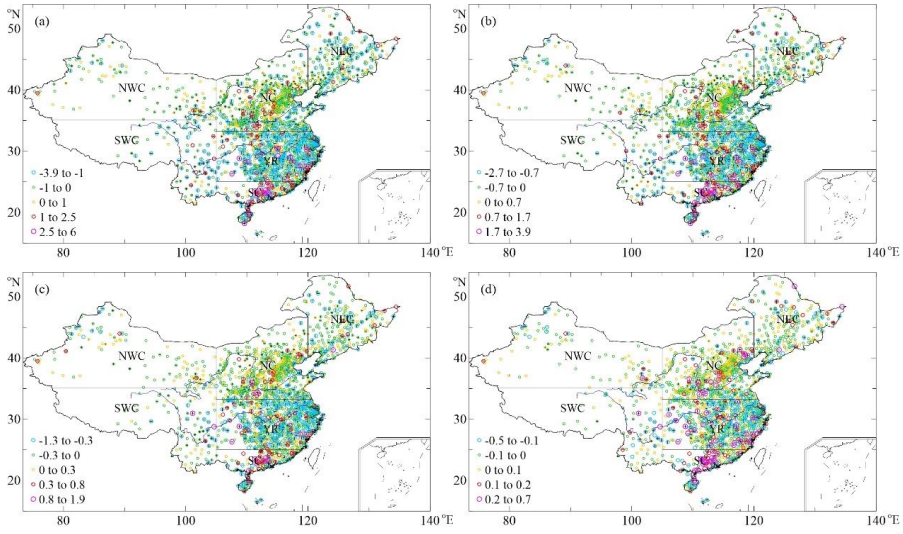

Figure 4. Spatial trends (Units: days per decade) of CWPDs frequencies at different thresholds in mainland China during 1981–2022. (a: W85∩P85; b: W90∩P90; c: W95∩P95; d: W98∩P98)

In mainland China, for the CWPDs frequencies during 1981-2022 under the threshold of W85∩P85, 76.8% of the stations showed decreased trends, 51.9% of the stations showed significant decreased trends, 23.2% of the stations showed increased trends, 7.9% of the stations showed significant increased trends. Under the threshold of W90∩P90, 74.8% of the stations showed decreased trends, 47.2% of the stations showed significant decreased trends, 25.2% of the stations showed increased trends, 9.6% of the stations showed significant increased trends. Under the threshold of W95∩P95, 73.5% of the stations showed decreased trends, 35.7% of the stations showed significant decreased trends, 26.3% of the stations showed increased trends, 6.3% of the stations showed significant increased trends, 0.2% of the stations showed stationary trend. Under the threshold of W98∩P98, 65.5% of the stations showed decreased trends, 19.0% of the stations showed significant decreased trends, 34.1% of the stations showed increased trends, 5.9% of the stations showed significant increased trends, 0.4% of the stations showed stationary trend (Table 1).

https://doi.org/10.5194/egusphere-2025-5893
Preprint. Discussion started: 4 December 2025

Table 1. Percentage of stations with variation trends and their significances for the frequency of CWPDs in mainland China (Units: %).

Thresholds	Positive trend			Negative trend			Stationary trend
	Total	SS	Non-SS	Total	SS	Non-SS	Total
W85∩P85	23.2	7.9	15.3	76.8	51.9	24.9	0.0
W90∩P90	25.2	9.6	15.6	74.8	47.2	27.6	0.0
W95∩P95	26.3	6.3	20.0	73.5	35.7	37.8	0.2
W98∩P98	34.1	5.9	28.2	65.5	19.0	46.5	0.4

SS: Trend is significant at the 0.05 level; Non-SS: Trend is not significant at the 0.05 level.

The percentage of stations with variation trends for the CWPDs frequencies during 1981-2022 under the threshold of W85∩P85 in six climate regions over mainland China were showed in Table 2. In NEC region, 77.9% of the stations showed decreased trends, 50.7% of the stations showed significant decreased trends, 22.1% of the stations showed increased trends, 7.4% of the stations showed significant increased trends. In NC region, 76.6% of the stations showed decreased trends, 45.3% of the stations showed significant decreased trends, 23.2% of the stations showed increased trends, 7.6% of the stations showed significant increased trends. In YR region, 81.2% of the stations showed decreased trends, 63.6% of the stations showed significant decreased trends, 18.8% of the stations showed increased trends, 5.7% of the stations showed significant increased trends. In SC region, 59.4% of the stations showed decreased trends, 36.2% of the stations showed significant decreased trends, 40.6% of the stations showed increased trends, 23.2% of the stations showed significant increased trends. In NWC region, 70.5% of the stations showed decreased trends, 36.6% of the stations showed significant decreased trends, 29.5% of the stations showed increased trends, 5.4% of the stations showed significant increased trends. In SWC region, 82.1% of the stations showed decreased trends, 70.2% of the stations showed significant decreased trends, 17.9% of the stations showed increased trends, 4.8% of the stations showed significant increased trends (Table 2).

Table 2. Percentage of stations with variation trends and their significances for the frequency of CWPDs (W85∩P85) in six climate regions over mainland China (Units: %).

Regions	Positive trend			Negative trend			Stationary trend
	Total	SS	Non-SS	Total	SS	Non-SS	Total
NEC	22.1	7.4	14.7	77.9	50.7	27.2	0.0
NC	23.2	7.6	15.6	76.6	45.3	31.3	0.2
YR	18.8	5.7	13.1	81.2	63.6	17.6	0.0
SC	40.6	23.2	17.4	59.4	36.2	23.2	0.0
NWC	29.5	5.4	24.1	70.5	36.6	33.9	0.0
SWC	17.9	4.8	13.1	82.1	70.2	11.9	0.0

https://doi.org/10.5194/egusphere-2025-5893
Preprint. Discussion started: 4 December 2025

SS: Trend is significant at the 0.05 level; Non-SS: Trend is not significant at the 0.05 level.

3.2 Characteristics of CWPDs intensity at different thresholds

In mainland China, different percentile thresholds had certain effects on the spatial pattern of the intensity of CWPDs. With the increase of the threshold, the range of CWPDs with stronger intensity further reduced. In general, CWPDs intensities were more severe in eastern coastal areas of YR, mid-eastern SC, parts of eastern SWC, parts of central NEC, parts of northwestern NWC and mid-northern in Hainan Province, but less serious in other areas, including most NEC, NWC and NC (Fig. 5).

Under the threshold of W85∩P85, annual mean CWPDs intensities were most severe in central SC, southeastern YR, several scattered areas in eastern SWC with value of 85 to 106.6, more severe in mid-eastern YR and SC, a little parts of eastern SWC, a little parts of northwestern NWC, a few scattered areas of mid-eastern NEC with value of 65 to 85, severe in parts of mid-eastern and western YR, parts of eastern SWC and southeastern SC, a little parts of northwestern NWC and mid-eastern NEC with value of 45 to 65 (Fig. 5a). Under the threshold of W90∩P90, the range of CWPDs with stronger intensity were similar to the threshold of W85∩P85. CWPDs intensities were most severe in central SC, southeastern YR, a few scattered individual areas of eastern SWC with value of 65 to 82, more severe in parts of mid-eastern YR, parts of central SC, some individual areas of eastern SWC and southeastern NC with value of 50 to 65, severe in parts of mid-eastern and western YR, parts of eastern SWC and southeastern SC, a little parts of northwestern NWC and mid-eastern NEC, parts of southeastern NC with value of 35 to 50 (Fig. 5b).

Under the threshold of W95∩P95, the range of CWPDs with stronger intensity had significantly decreased compared to the threshold of W90∩P90. Annual mean CWPDs intensities were most severe in a few individual areas of southeastern NWC with value of 70 to 92.3, more severe in several areas of central SC, several areas of southeastern YR and eastern SWC with value of 50 to 70, severe in parts of mid-southern SC, parts of eastern YR and western YR, a little parts of southeastern NWC, a little parts of southeastern NC and central NEC with value of 35 to 50 (Fig. 5c). Under the threshold of W98∩P98, the range of CWPDs with stronger intensity were similar to the threshold of W95∩P95. CWPDs intensities were most severe in several stations of eastern SWC and mid-eastern YR with value of 60 to 77.8, more severe in individual stations of mid-eastern YR and SC, several stations of central NWC and NEC with value of 45 to 60, severe in parts of mid-southern SC, parts of mid-eastern and western YR, several scattered areas of southeastern SWC, several scattered areas of northwestern and southeastern NWC, a few scattered areas of mid-southern NC and NEC with value of 30 to 45 (Fig. 5d).

https://doi.org/10.5194/egusphere-2025-5893
Preprint. Discussion started: 4 December 2025

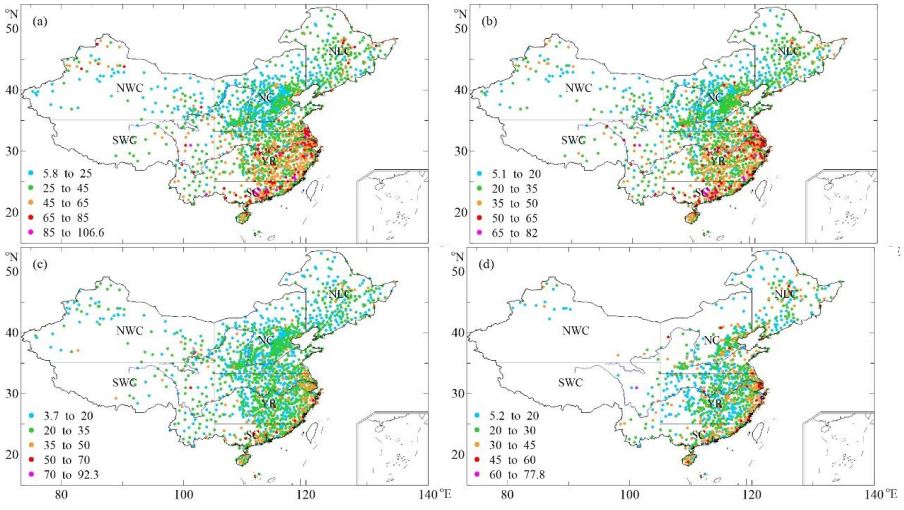

Figure 5. Annual average (Units: unitless per year) of CWPDs intensity at different thresholds in mainland China during 1981–2022. (a: W85∩P85; b: W90∩P90; c: W95∩P95; d: W98∩P98)

Inter-annual changes of CWPDs intensity of four different thresholds in mainland China during 1981–2022 were showed in Fig. 6. As shown in the figure, with the increase of the threshold, the weakening trends of annual CWPDs intensities further weakened and even slightly strengthened during 1981-2022. During 1981-2010, the CWPDs intensities under four different thresholds all showed weakened trends, but during 2011-2022, the CWPDs intensities under four different thresholds all showed enhanced trends.

Under the threshold of W85∩P85, annual mean CWPDs intensities decreased significantly at a rate of 3.59 per decade in the past 42 years. During 1981-2010, the CWPDs intensities weakened significantly with a speed of 7.67 per decade, during 2011-2022, the CWPDs intensities increased significantly with a speed of 9.56 per decade (Fig. 6a). Under the threshold of W90∩P90, annual mean CWPDs intensities decreased significantly at a rate of 1.47 per decade in the past 42 years. During 1981-2010, the CWPDs intensities weakened significantly with a speed of 4.60 per decade, during 2011-2022, the CWPDs intensities enhanced significantly with a speed of 8.45 per decade (Fig. 6b).

Under the threshold of W95∩P95, annual mean CWPDs intensities weakened non-significantly at a rate of 0.07 per decade during 1981-2022. During 1981-2010, the CWPDs intensities weakened significantly with a speed of 2.23 per decade, during 2011-2022, the CWPDs intensities increased significantly with a speed of 5.68 per decade (Fig. 6c). Under the threshold of W98∩P98, annual mean CWPDs intensities increased non-significantly at a rate of 0.01 per decade in the past 42 years. During 1981-2010, the CWPDs intensities weakened significantly with a speed of 1.03 per decade, during 2011-2022, the CWPDs intensities increased non-significantly with a speed of 0.58 per decade (Fig. 6d).

https://doi.org/10.5194/egusphere-2025-5893
Preprint. Discussion started: 4 December 2025

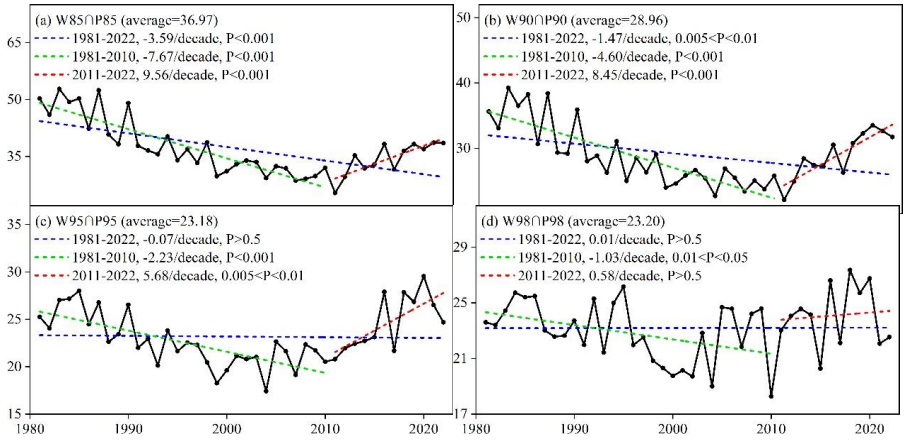

Figure 6. Inter-annual changes of CWPDs intensity at different thresholds in mainland China during 1981–2022.

From 1981 to 2022, The CWPDs intensities under the four thresholds all showed decreasing trends in most areas of mainland China except for parts of central SC, a few scattered areas of YR, several scattered areas of NC and NEC, a few scattered areas of NWC, individual areas of eastern SWC. In most areas of mainland China, as the thresholds increased, the trends of weakened for CWPDs intensities decreased and the scopes with a slight strengthening trend expanded (Fig. 7). Under the threshold of W85∩P85, the CWPDs intensities decreased most obviously at rates of 20-47.1 per decade mainly occurred in several stations of eastern SWC and northern NEC, several stations of northwestern and southeastern NWC. The decreasing trends of 10-20 per decade of CWPDs intensities mainly occurred in most YR, eastern SWC, and mid-eastern NEC. The increasing trends of 20-38.2 per decade of CWPDs intensities mainly occurred in central SC, several scattered stations of YR, several stations of eastern SWC. The increasing trends of 0-20 per decade of CWPDs intensities mainly occurred in parts of central NC, parts of mid-southern NWC and NEC (Fig. 7a). Under the threshold of W90∩P90, the CWPDs intensities increased more obviously at rates of more than 10 per decade in parts of central SC and mid-southern YR, several areas of eastern SWC, several regions of southeastern NWC and central NC. The more obvious decreasing trends of 10-28 per decade occurred in most YR, parts of mid-southern NEC, a little parts of northwestern NWC, parts of mid-eastern SWC, a little parts of southeastern NC. The regions showed decreasing trend with rates of 0-10 per decade widely distributed in NC and YR, some parts of eastern and southern SC, some parts of central and eastern SWC, some scattered areas of NWC and NEC. In other areas, the CWPDs intensities showed rising trends of 0-10 per decade (Fig. 7b).

Under the threshold of W95∩P95, the stations number with increased trends of CWPDs intensities significantly increased compared to the threshold of W90∩P90, especially in the YR region. The CWPDs intensities increased more obviously at rates of more than 10 per decade in several stations of central SC, several stations of southern and western YR, several stations of central NC, several stations of southeastern NWC and eastern SWC. The most obvious decreasing trends of 10-23.5 per decade

https://doi.org/10.5194/egusphere-2025-5893
Preprint. Discussion started: 4 December 2025

mainly occurred in a few areas of northern and western YR, several stations of mid-eastern NEC, several stations of northwestern and southern NWC (Fig. 7c). Under the threshold of W98∩P98, the scopes with increased trends of CWPDs intensities further increased compared to the threshold of W95∩P95. The CWPDs intensities increased more obvious with a speed of 10-20 per decade occurred in several scattered stations of northern and southern YR, a few stations of southern NC, several stations of eastern SWC and central NEC. The most obvious increasing trends of 20-36.7 per decade occurred in several stations of northern SC, several stations of northern YR and eastern SWC. The most obvious decreasing trends of 20-32.9 per decade mainly occurred in several stations of southwestern and northwestern YR, several stations of northwestern NEC (Fig. 7d).

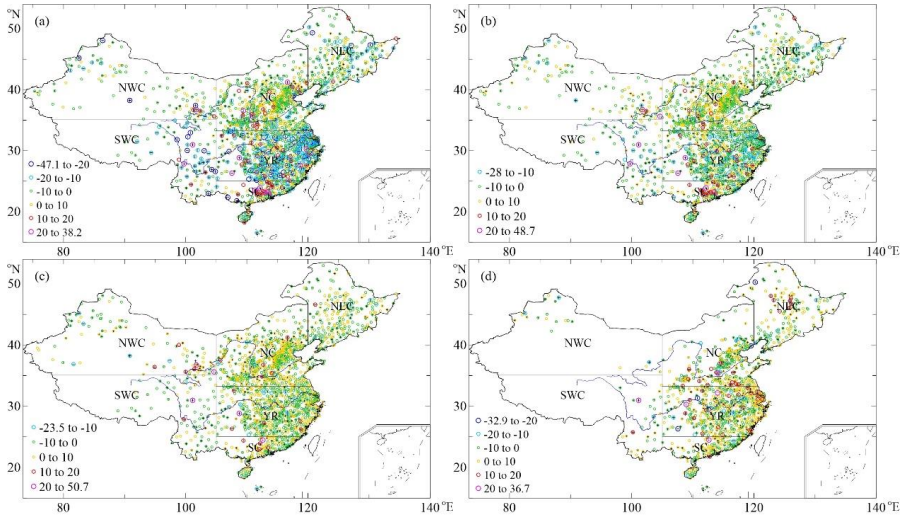

Figure 7. Spatial trends (Units: unitless per decade) of CWPDs intensity at different thresholds in mainland China during 1981–2022. (a: W85∩P85; b: W90∩P90; c: W95∩P95; d: W98∩P98)

In mainland China, for the CWPDs intensities during 1981-2022 under the threshold of W85∩P85, 73.8% of the stations showed decreased trends, 41.7% of the stations showed significant decreased trends, 26.2% of the stations showed increased trends, 7.7% of the stations showed significant increased trends. Under the threshold of W90∩P90, 70.1% of the stations showed decreased trends, 32.4% of the stations showed significant decreased trends, 29.9% of the stations showed increased trends, 9.5% of the stations showed significant increased trends. Under the threshold of W95∩P95, 59.8% of the stations showed decreased trends, 22.7% of the stations showed significant decreased trends, 40.2% of the stations showed increased trends, 13.2% of the stations showed significant increased trends. Under the threshold of W98∩P98, 51.1% of the stations showed decreased trends, 24.0% of the stations showed significant decreased trends, 48.9% of the stations showed increased

https://doi.org/10.5194/egusphere-2025-5893
Preprint. Discussion started: 4 December 2025

trends, 24.0% of the stations showed significant increased trends (Table 3).

Table 3. Percentage of stations with variation trends and their significances for the intensity of CWPDs in mainland China (Units: %).

Thresholds	Positive trend			Negative trend			Stationary trend
	Total	SS	Non-SS	Total	SS	Non-SS	Total
W85∩P85	26.2	7.7	18.5	73.8	41.7	32.1	0.0
W90∩P90	29.9	9.5	20.4	70.1	32.4	37.7	0.0
W95∩P95	40.2	13.2	27.0	59.8	22.7	37.1	0.0
W98∩P98	48.9	24.0	24.9	51.1	24.0	27.1	0.0

SS: Trend is significant at the 0.05 level; Non-SS: Trend is not significant at the 0.05 level.

The percentage of stations with variation trends for the CWPDs intensities during 1981-2022 under the threshold of W85∩P85 in six climate regions over mainland China were showed in Table 4. In NEC region, 77.0% of the stations showed weakened trends, 42.0% of the stations showed significant weakened trends, 23.0% of the stations showed enhanced trends, 5.5% of the stations showed significant enhanced trends. In NC region, 69.9% of the stations showed weakened trends, 32.1% of the stations showed significant weakened trends, 30.1% of the stations showed enhanced trends, 8.0% of the stations showed significant enhanced trends. In YR region, 78.3% of the stations showed weakened trends, 55.7% of the stations showed significant weakened trends, 21.7% of the stations showed enhanced trends, 6.6% of the stations showed significant enhanced trends. In SC region, 62.3% of the stations showed weakened trends, 26.8% of the stations showed significant weakened trends, 37.7% of the stations showed enhanced trends, 16.7% of the stations showed significant enhanced trends. In NWC region, 73.2% of the stations showed weakened trends, 28.6% of the stations showed significant weakened trends, 26.8% of the stations showed enhanced trends, 5.4% of the stations showed significant enhanced trends. In SWC region, 83.3% of the stations showed weakened trends, 59.5% of the stations showed significant weakened trends, 16.7% of the stations showed enhanced trends, 7.2% of the stations showed significant enhanced trends (Table 4).

Table 4. Percentage of stations with variation trends and their significances for the intensity of CWPDs (W85∩P85) in six climate regions over mainland China (Units: %).

Regions	Positive trend			Negative trend			Stationary trend
	Total	SS	Non-SS	Total	SS	Non-SS	Total
NEC	23.0	5.5	17.5	77.0	42.0	35.0	0.0
NC	30.1	8.0	22.1	69.9	32.1	37.8	0.0
YR	21.7	6.6	15.1	78.3	55.7	22.6	0.0
SC	37.7	16.7	21.0	62.3	26.8	35.5	0.0
NWC	26.8	5.4	21.4	73.2	28.6	44.6	0.0

https://doi.org/10.5194/egusphere-2025-5893
Preprint. Discussion started: 4 December 2025

SWC	16.7	7.2	9.5		83.3	59.5	23.8		0.0

SS: Trend is significant at the 0.05 level; Non-SS: Trend is not significant at the 0.05 level.

3.3 Dependence of concurrent days on individual ones

During 1981–2022, extreme wind speed days decreased significantly at the rate of 10.13 days per decade and extreme precipitation days increased significantly at the rate of 0.74 days per decade. Extreme wind speed days decreased significantly at a speed of 16.30 days per decade during 1981–2010, and then increased significantly at a rate of 13.64 days per decade. Extreme precipitation days increased non-significantly with a speed of 0.33 days per decade during 1981–2010, and increased non-significantly at a speed of 2.01 days per decade during 2011–2022. It could be seen that, precipitation had a more obvious increasing trend after 2010 (Fig. 8a), which is consistent with the results of Zhang et al. (2021).

The ratio of CWPDs to extreme wind speed days declined significantly with a rate of 1.32% per decade during 1981–2022. The ratio increased significantly with a rate of 1.04% per decade during 1981–2010, and increased non-significantly at a rate of 1.01% per decade during 2011–2022. For extreme precipitation days, the ratio decreased significantly at a rate of 4.21% per decade in the past 42 years. The ratio of CWPDs to extreme precipitation days decreased significantly at a rate of 6.69% per decade during 1981–2010, and then increased significantly at a rate of 6.47% per decade during 2011–2022. It can be seen that before 2010, the number of extreme wind speed days decreased significantly, resulting in an increase in the ratio of CWPDs to extreme wind speed days, but after 2010, the number of CWPDs increased significantly (Fig. 3a), resulting in an increase in the ratio of CWPDs to extreme wind speed days. Contrastively, after 2010, the number of CWPDs increased significantly (Fig. 3a), leading to a rapid increase in the ratio of CWPDs to extreme precipitation days (Fig. 8b).

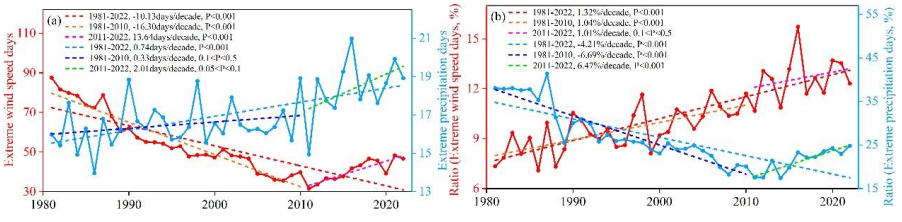

Figure 8. Inter-annual variations of extreme wind speed days (W85), extreme precipitation days (P85) (a) and the ratio of CWPDs (W85∩P85) frequencies to individual extreme wind speed or extreme precipitation days (b).

Spatially, the ratio of CWPDs to extreme wind speed days increased at a rate of 0-10% per decade in most areas from 1981 to 2010, increased at a rate of more than 10% per decade only occurred in several stations of northern and southeastern YR, and several stations of southern of Hainan Province, and the regions where the ratio decreased mainly occurred in northern and western NC, parts of southeastern NWC, northeastern SWC, southwestern NEC, and a few scattered stations of YR (Fig. 9a). Meanwhile, the ratio of CWPDs to extreme precipitation days showed a decreasing trend in most of the country, and a more obviously increased trend with rate of 10-22.8% per decade only showed in a few scatter stations in central SC and NC, and northern YR (Fig. 9c). During 2011–2022, the scope of the ratio of CWPDs to extreme wind speed days showing a downward trend expanded compared to the

https://doi.org/10.5194/egusphere-2025-5893
Preprint. Discussion started: 4 December 2025

period of 1981-2010, the greatest downward trend of the ratio included several stations of southern and western SC, several stations of southeastern SWC, several stations of northwestern NC, and the areas with greatest increasing trend mainly appeared in parts of northeastern and northern YR, parts of southeastern NC, and parts of western NEC (Fig. 9b). The scopes of the ratio of CWPDs to extreme precipitation days showing an increasing trend expanded compared to the period of 1981-2010 in most areas, indicating that the increased rates of CWPDs more than the increased rates of extreme precipitation days in most areas. The decrease of the ratio was mainly distributed in parts of eastern SWC, parts of southeastern SC, some scattered areas in YR, parts of northern NC and southern NEC and central NWC, indicating that the precipitation in these regions tended to increase or CWPDs tended to decrease (Fig. 9d).

In conclusion, from 1981 to 2010, the areas with decreasing extreme wind speed days were more widely distributed, while the regions with increasing extreme precipitation days were more widely distributed. During 2011–2022, the areas with the increase of extreme wind speed days were more widely distributed, the increased rates of CWPDs more than the increased rates of extreme precipitation days were widely distributed. The distribution of CWPDs trends was relatively consistent with that of extreme wind speed days during the two periods, but the trend value of CWPDs was smaller than that of extreme wind speed days.

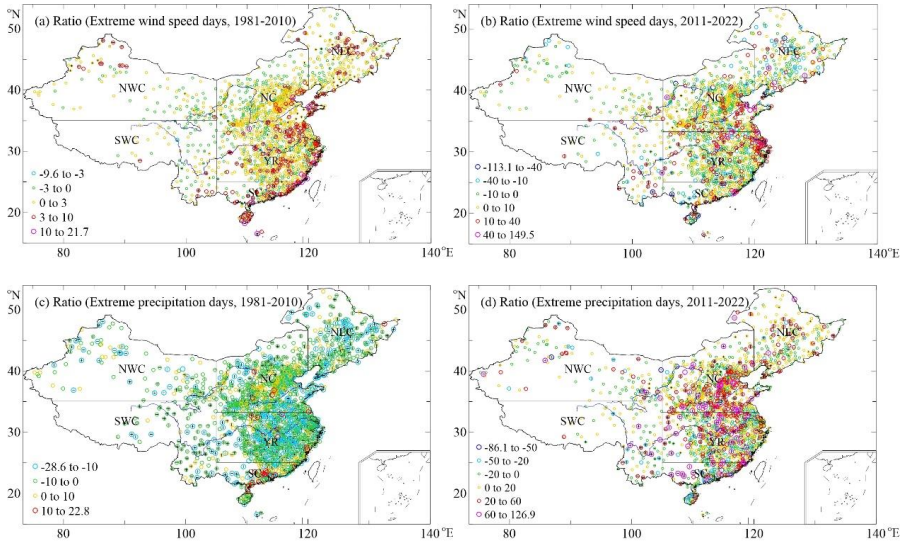

Figure 9. Spatial trends of ratio of CWPDs (W85∩P85) frequencies to extreme wind speed days (a, b) and extreme precipitation days (c, d) during 1981–2010 and 2011–2022.

During 1981–2010, CWPDs decreased in most parts of the country, among which the decreasing trend of CWPDs was the largest in parts of eastern SWC, parts of central SC, and some scatter regions of YR, with the rate of 4-6.6 days per decade (Fig. 10a). CWPDs showed a most obvious increasing trend only in parts of central SC, a few scattered stations of YR, with the rate of 2-4.5 days per decade. The scopes of CWPDs showing an increasing trend expanded obviously compared to the period of

https://doi.org/10.5194/egusphere-2025-5893
Preprint. Discussion started: 4 December 2025

1981-2010 in most areas of the country, among which CWPDs in parts of western and southern SC, several stations eastern SWC, some scattered stations in western and central YR, a few stations of southern NC, several stations of southeastern NWC showed an increasing trend of 15-42.1 days per decade, which was significantly higher than that in 1981–2010 (Fig. 10b). In parts of southern SC, mid-western of Hainan Province, some scattered stations of central and southern YR, parts of eastern SWC, a few scattered areas of mid-southern NEC, central and western NC, central and eastern NEC and central SC, CWPDs showed a decreasing trend. In general, the region of YR showed the most obvious change from the obvious decreased during 1981-2010 to the obvious increased during 2011-2022.

The spatial trend of extreme wind speed days during 1981–2010 and 2011–2022 was consistent with that of CWPDs, though the value of the latter was obviously greater than that of CWPDs (Fig. 10c and 10d). The trend of extreme precipitation days in the period of 1981-2010 lacked obvious correspondence with that of CWPDs (Fig. 10e). From 1981 to 2010, extreme precipitation days increased more obviously at a rate of 1-4 days per decade mainly in southeastern NEC, parts of central and southeastern NC, parts of southeastern and northwestern NWC, a little parts of central and eastern YR, a little parts of central and eastern SWC (Fig. 10e). During 2011–2022, the areas with the most pronounced increase in extreme precipitation days had shifted significantly to the south, and the scope that extreme precipitation days showed an increasing trend widened further, with the increase in extreme precipitation days in most regions and the prominent upward trend (Fig. 10f). Only in northwestern NWC, the Beijing-Tianjin-Hebei region and southeastern YR, extreme precipitation days decreased obviously.

https://doi.org/10.5194/egusphere-2025-5893
Preprint. Discussion started: 4 December 2025

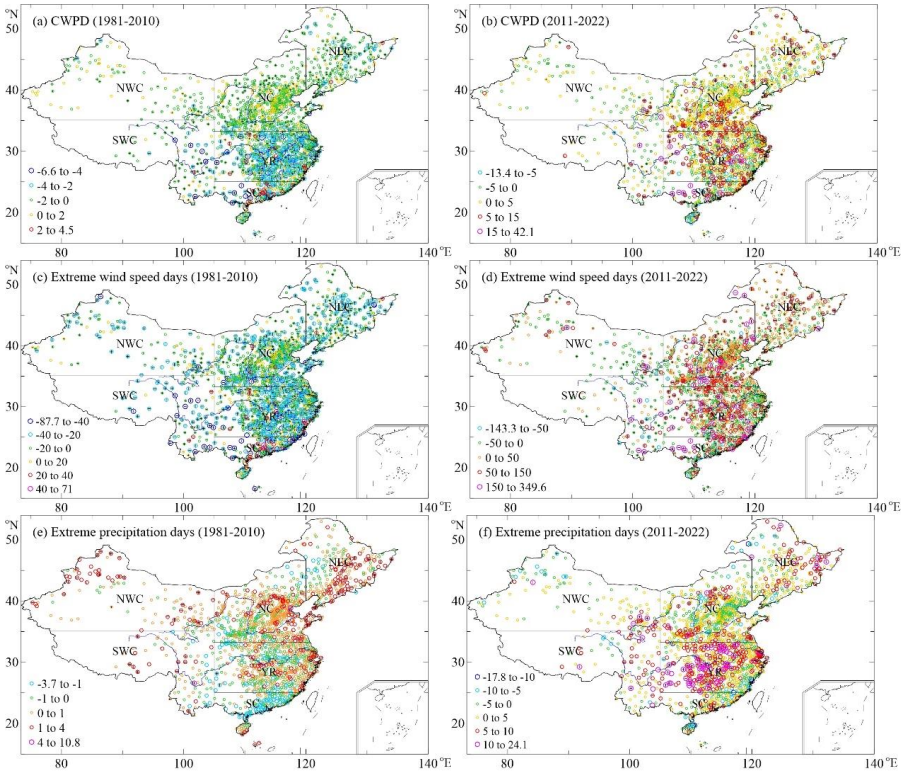

Figure 10. Spatial trends (Units: days per decade) of CWPDs (W85∩P85) frequencies (a, b), extreme wind speed days (W85) (c, d) and extreme precipitation days (P85) (e, f) during 1981–2010 and 2011–2022. Positive sign denotes the trends passing the 0.05 significance level, the same as below.

4 Discussion

The most common approach to define a compound extreme wind speed and extreme precipitation day is to determine a fixed percentile threshold of extreme wind speed day or extreme precipitation day for the year or a specific season (Zhang et al., 2021; Zscheischler et al., 2021). Whereas, in the context of global warming, extreme wind speed days and extreme precipitation days also show an increasing or decreasing trend, therefore, a time-varying daily threshold need to be adopted. In this study, a time-varying daily threshold was defined by using the daily maximum wind speed and precipitation observation data of 1686 meteorological stations covering most areas of mainland China, and the change characteristics of CWPDs under different percentile thresholds were investigated in mainland China from 1981 to 2022.

The variations in individual extreme speed wind and extreme precipitation day imposed different influences on the CWPDs. For instance, the frequencies of CWPDs identified by the 90th percentile of daily maximum wind speed and the 90th percentile of daily precipitation (Fig. 2b) were comparable to those identified by the 85th percentile of maximum wind speed and the 85th percentile of precipitation (Fig. 2a), but the former resulted in smaller frequencies than the latter in almost all regions. The

https://doi.org/10.5194/egusphere-2025-5893
Preprint. Discussion started: 4 December 2025

characteristics of the probability distribution of two (or more) individual hazards or extremes appear to play a key role in compound extremes. Zscheischler et al. (2020) also pointed out that variations in the deviation or the change in the mean of an individual hazard or extreme could affect the changes of the concurrent event. In general, southeastern SC, Hainan Province, northwestern YR, some scattered areas in the central and eastern YR were areas where the CWPDs were frequent, and CWPDs were less in most of NWC, SWC, NEC and NC (Fig. 2).

Although CWPDs frequencies decreased in mainland China before 2010, and showed an obvious increasing trend after 2010 caused by the increases in extreme wind speed days from 2011 to 2022 (Fig. 3 and Fig. 8). We found that the variations in CWPDs were more consistent with those of extreme wind speed days (Fig. 8a), both decreasing in 1981-2010, and increasing in 2011–2022. This in line with the finding of Zhang et al. (2021). From 1981 to 2022, The CWPDs frequencies under the four thresholds all showed decreasing trends in most areas of mainland China. As the threshold increased, the trends of decreased for CWPDs frequencies decreased (Fig. 4).

CWPDs directly drived by synoptic factors such as cyclones and atmospheric rivers (ARs). In the subtropics and midlatitudes areas, the precipitation and wind extremes are often related to cyclones (Raveh-Rubin and Wernli, 2015). Regional variations in the coexistence of the extremes are owing to differences in the relative positioning of the cyclone centers and the extremes. For instance, both spring extreme precipitation and wind events in the region of the middle and lower reaches of the Yangtze River and the Huai River Basin are typically associated with Jianghuai cyclones, such that the same low-pressure system can induce both types of weather extremes in this region (Zhu and Chen, 2024). The Yellow River cyclone is a significant precipitation weather system in the northeastern China during summer, often causing heavy rain in the southern part of the region (Miao et al., 2015), the summer strong winds in the region can be caused by the cold air from the north, which periodically moves southward as a cold front. Hence, different weather systems are responsible for precipitation and wind extremes and as a result the number of cooccurrence extremes is lower. Li et al. (2022) found that the CWPDs in the coastal areas of NC tend to be associated with tropical cyclones (TCs) accompanied by atmospheric rivers, which is possibly due to a poleward shift in storm tracks (Wang et al., 2013), the decreasing trends of the frequency of summer CWPDs in SC caused by the decreasing trends of ARs-related and cyclone-ARs-related events during 1979 to 2020, CWPDs in SC showed decreasing trends for frequency and intensity in winter related to the decreasing of ARs and cyclone-ARs events. This is agree with our findings that the decreasing trends of the frequency and intensity of CWPDS in

https://doi.org/10.5194/egusphere-2025-5893
Preprint. Discussion started: 4 December 2025

this region (Fig. S1 and S2). CWPDs in Hainan province in summer are mainly caused by cyclone. The CWPDs occurrence in parts of northern inland China in summer, and central and southern China in winter were dominated by the landfalling ARs (Li et al., 2022). Many previous studies also pointed out that more frequent TC occurrences associated with intense precipitation under warming conditions (Knutson et al., 2020; Yamaguchi et al., 2020; Yaddanapudi et al., 2022) in different regions, such as in southeast China (Lui et al., 2019). Sussman et al. (2020) indicated that large-scale atmospheric Rossby wave activities may contribute to CWPDs in the midlatitudes.

Furthermore, topographic effects also cause regional variations in wind and precipitation extremes. For example, the precipitation on the northern slope of the Tianshan Mountains is greater than that on the southern slope. Due to the gap in the northwest of the Junggar Basin, the northern slope of the Tianshan Mountains is influenced by water vapor from the Atlantic Ocean and the Arctic Ocean, resulting in more precipitation. The northern slope of the Tianshan Mountains is a windward slope and has an uplifting effect on water vapor, hence more precipitation. The southern slope of the Tianshan Mountains is a leeward slope and is deep inland, making it difficult for oceanic water vapor to reach, so there is less precipitation. The northern slope of the Tianshan Mountains is prone to being influenced by the westerly and northerly winds coming from the Atlantic Ocean and the Arctic Ocean. The topography of the northern slope of the Tianshan Mountains may cause it to experience the "constriction effect" in certain circumstances, where the wind speed increases in the narrow passage. This can also lead to an increase in wind speed in local areas (Chen et al., 2018).

In some cases, foehn effects with strong precipitation happening on the windward side and very strong downslope winds in the lee of the mountains. In the Tianshan Mountains, the weak moisture from the Arctic Ocean and the Atlantic Ocean is blocked by the Tianshan Mountains and is lifted upwards. At the mountain foothills, it forms more precipitation. After the air current passes over the mountains and descends, the katabatic wind effect intensifies the drought in the Tarim Basin (Ayitken et al., 2022). In this cases, heavy precipitation occurred only on the windward side of the mountains, while the extreme winds extended much farther northward. In other areas, local dry and intense wind systems tied to large-scale weather conditions and specific orographic settings explain the low frequencies of extreme wind and precipitation events. For example, the low-frequency events in Qinghai-Tibet Plateau, Inner Mongolia Plateau, Loess Plateau might be linked to northwest wind and high altitude. In these areas, due to its location within the Eurasian continent and its distance from the

https://doi.org/10.5194/egusphere-2025-5893
Preprint. Discussion started: 4 December 2025

sea, it is less affected by the summer winds. The moist oceanic air currents are blocked by the mountains and thus cannot penetrate deeply, and the strong and dry cold wave occur several times every winter (Zhang et al., 2007).

Ding et al. (2020) pointed out that the average wind speed across the country decreased at a rate of 0.1-0.22m/s per decade from 1961 to 2016, this is consistent with our result. Urbanization and land use has been proven to significantly affect the surface wind speed in China. Chen (2013) calculated that the difference in wind speed change rates between urban stations and rural stations resulted in a contribution rate of approximately 18% for urbanization in China's major cities to the reduction of wind speed. The increase in ground drag force will also significantly reduce the wind speed near the ground. The increase in ground drag force is mainly due to the change in the underlying surface (surface roughness). Climate warming has led to an increase in vegetation coverage in the mid-to-high latitudes of the globe, resulting in an increase in surface roughness and being an important factor contributing to the increase in ground drag force (Ding et al., 2020). Under the background of climate warming, the weakening of the thermal/pressure gradient force in the lower part of the troposphere, which also serves as the main driving force, is a key factor leading to the reduction of ground wind speed (Guo et al., 2011; Zhou et al., 2017). Xiong et al. (2019) demonstrated that the north-south pressure gradient decreased, Resulting in the weakening of the northwest wind speed in autumn in China. Zhou et al. (2017) pointed out that the simultaneous reduction of land-sea thermal differences and north-south thermal differences will undoubtedly lead to the synchronous weakening of the east-west and north-south pressure gradient forces, thereby reducing the ground wind speed. China is located in a typical monsoon region, and the variation of surface wind speed is also largely determined by the East Asian monsoon (Ding et al., 2020). Otherwise, the synergy between PDO and the Atlantic Multidecadal Oscillation (AMO) is the main driving factor for the 30-40-year oscillation of the East Asian summer monsoon (Ding et al., 2018; Ding and Li, 2016). Shi and Xu (2007) through conducting sensitivity tests using regional climate models also indicate that the interdecadal weakening of the East Asian winter monsoon might be related to the interdecadal warming in the eastern part of the East Asian continent. Although the East Asian winter monsoon does not exactly match the changing trend of the winter ground wind speed in China, it still has a significant impact. Most studies suggest that global warming has an enhancing effect on the East Asian summer monsoon (Jiang and Tian, 2013; Sun and Ding, 2011; Chen et al., 2019).

https://doi.org/10.5194/egusphere-2025-5893
Preprint. Discussion started: 4 December 2025

Aerosols also contribute to the weakening of the East Asian monsoon (Wu et al., 2015). Unlike greenhouse gases which favor the strengthening of the low-level circulation, aerosols mainly have a weakening effect on the low-level circulation, this is because the surface cooling effect caused by aerosols reduces the sea-land temperature difference, and the influence of the mutual conversion of potential and kinetic energy (Ma et al., 2018). Liu et al. (2019) also found that the sulfate aerosol emissions in the Northern Hemisphere might be the main factor leading to the unprecedented weakening of the East Asian summer monsoon.

Lots of previous studies have confirmed that large-scale climate factors have a close relationship with precipitation extremes. Pu et al. (2024) found that during the developing summer, El Niño mainly affected eastern China, resulting in extreme precipitations in Northern China, extreme precipitations decreased in the Jiangnan region, but increased significantly in the Jianghuai region. Liu et al. (2018) found that during the year when the super El Niño event weakened, the probability of extreme precipitation events significantly increased throughout eastern China, especially in areas north of the Jianghuai region, in the summer of the same year, the probability of extreme precipitation in the Yangtze River Basin was nearly twice as high as in normal years, while it decreased relatively in the southern and northern regions of China. Wu et al. (2016) found that the long-term trend of the annual extreme precipitation index indicates that most of the extreme precipitation indices show an increasing trend in the northwest and middle reaches of the Yangtze River region (except for consecutive dry days), as well as in the southeast coast and most areas of southern China, however, in the north China region, it shows a decreasing trend, since 2000, most of the indices have shown varying degrees of increasing trends, meaning that extreme precipitation events have become more frequent since 2000, this is consistent with our findings. Wang et al. (2021) showed that when El Niño occurs in winter, the intensity of extreme precipitation in autumn in the eastern coastal areas of China, and the lower reaches areas of the Yellow and the Yangtze Rivers, will increase by 26% in the following year, when La Niña occurs in winter, the intensity of extreme precipitations in spring and summer in eastern China will increase by 8.8% and 5.1% respectively in the following year, when NAO is in a positive phase, the frequency of extreme precipitations in spring, summer and autumn is relatively high in most areas of China, and the intensity of summer extreme precipitations in East China increases by 8.5%. Chen et al. (2022) showed that the southwestern region generally showed an increasing trend in precipitation frequency and intensity, as well as an increase in extreme precipitation from 1969 to 2020, and the

https://doi.org/10.5194/egusphere-2025-5893
Preprint. Discussion started: 4 December 2025

extreme precipitation index in the southwestern region is closely related to strong ENSO events. Furthermore, the impact of urbanization on extreme precipitation is also increasing (Wan et al., 2013). Therefore, the variation of CWPDs were simultaneously influenced by multiple combinations of large-scale climate modes and anthropogenic warming, such as urbanization and land use.

In mainland China, different percentile thresholds had certain effects on the spatial pattern of the intensity of CWPDs. With the increase of the threshold, the range of CWPDs with stronger intensity further reduced. The CWPDs intensities were more severe in eastern coastal areas of YR, mid-eastern SC, parts of eastern SWC, parts of central NEC, parts of northwestern NWC and mid-northern in Hainan Province (Fig. 5). Annual CWPDs intensities changed obvious around early-to-mid 2010s in under four different thresholds. With the increase of the threshold, the weakening trends of annual CWPDs intensities further weakened and even slightly strengthened during 1981-2022. During 1981-2010, the CWPDs intensities under four different thresholds all showed weakened trends, but during 2011-2022, the CWPDs intensities under four different thresholds all showed enhanced trends (Fig. 6). From 1981 to 2022, the CWPDs intensities under the four thresholds all showed decreasing trends in most areas of mainland China except for parts of central SC, a few scattered areas of YR, several scattered areas of NC and NEC, a few scattered areas of NWC, individual areas of eastern SWC. As the thresholds increased, the trends of weakened for CWPDs intensities decreased and the scopes with a slight strengthening trend expanded (Fig. 7). This indicated that high-intensity composite wind speed and precipitation extremes have occurred frequently in the past few decades, especially in eastern coastal areas of YR, mid-eastern SC, parts of eastern SWC and mid-northern in Hainan Province, such incidents coupled with high exposure and vulnerability of the population or crops, causing huge losses in multiple aspects including water security, food security and human health. Therefore, it is necessary to enhance climate adaptability or resilience in these regions, such as increasing water conservancy development in agricultural areas, change the agricultural production mode, and introduce drought-resistant and heat-tolerant crop varieties.

In this study, we mainly concentrated on the wind speed and precipitation extremes that occur on the same day, namely, the concurrent extreme wind speed and extreme precipitation days, as compound extremes are more devastating and damaging than independent extreme event. Compound wind speed and precipitation extremes are not just phenomena that occur on the same day, and other forms should also be addressed. For instance, extreme wind speed or extreme precipitation occurs a day or two after

https://doi.org/10.5194/egusphere-2025-5893
Preprint. Discussion started: 4 December 2025

or before CWPDs (Zscheischler et al., 2020), wind speed and precipitation extremes appear in a relatively short period of time in nearby regions (Raymond et al., 2020), and so on. Moreover, the physical process diagnosis, change attribution, risk quantification and adaptation measures of CWPDs are also not involved in this paper, which need to be explored in future studies.

5 Conclusions

In mainland China, CWPDs were more frequent in southeastern South China, Hainan Province, the northwestern parts of the middle and lower reaches of Yangtze River, some scattered areas in the central and eastern YR. Annual CWPDs decreased in mainland China during 1981–2010, and then showed an obvious upward trend after 2010. Different percentile thresholds had effects on the spatial pattern and change trend of CWPDs. From 1981 to 2022, The CWPDs frequencies under the four thresholds all showed decreasing trends in most areas of mainland China. As the threshold increased, the trends of decreased for CWPDs frequencies decreased.

In mainland China, different percentile thresholds had certain effects on the spatial pattern of the intensity of CWPDs. With the increase of the threshold, the range of CWPDs with stronger intensity further reduced. The CWPDs intensities were more severe in eastern coastal areas of YR, mid-eastern SC, parts of eastern SWC, parts of central NEC, parts of northwestern NWC and mid-northern in Hainan Province. Annual CWPDs intensities changed obvious around early-to-mid 2010s in under four different thresholds. With the increase of the threshold, the weakening trends of annual CWPDs intensities further weakened and even slightly strengthened during 1981-2022. During 1981-2010, the CWPDs intensities under four different thresholds all showed weakened trends, but during 2011-2022, the CWPDs intensities under four different thresholds all showed enhanced trends. From 1981 to 2022, the CWPDs intensities under the four thresholds all showed decreasing trends in most areas of mainland China except for parts of central SC, a few scattered areas of YR, several scattered areas of NC and NEC, a few scattered areas of NWC, individual areas of eastern SWC. As the thresholds increased, the trends of weakened for CWPDs intensities decreased and the scopes with a slight strengthening trend expanded.

After 2010, the number of CWPDs increased significantly, resulting in an increase in the ratio of CWPDs to extreme wind speed days and a rapid increase in the ratio of CWPDs to extreme precipitation days. The changes of extreme wind speed days were consistent with those of CWPDs during 1981–2010 and 2011–2022, but the change of extreme precipitation days lacked correspondence with that of CWPDs in the two periods, especially in the previous period.

https://doi.org/10.5194/egusphere-2025-5893
Preprint. Discussion started: 4 December 2025

Data availability. Two long-term daily historical observation datasets of daily maximum wind speed and daily total precipitation from 1686 meteorological stations over mainland China may be accessed at http://data.cma.cn/.

Author contributions. JS conceptualized the research idea and objective. KW and JS developed the research methodology. KW carried out the document analysis and wrote the initial draft. Both authors repeatedly reviewed and edited the following draft versions.

Competing interests. The contact author has declared that neither of the authors has any competing interests.

Financial support. This work was supported by the Natural Science Foundation of Shanghai (No. 23ZR1456900), National Key Research and Development Program of China (No. 2023YFC3805304-1) and Climate Change Project of China Meteorological Administration (No. QBZ202412).

References

Ayitken, M., Li, X., Musa, Y., et al.: Temporal and Spatial Characteristics of Foehn on the North Slope of the Tianshan Mountains of China and Prediction Ability of European Fine Grid Numerical Products, Mountain Research, 40, 823-834, doi:10.16089/j.cnki.1008-2786.000716, 2022.

Alizadeh, M. R., J. Adamowski, M. R. Nikoo, A. AghaKouchak, P. Dennison, and Sadegh, M.: A century of observations reveals increasing likelihood of continental-scale compound dry-hot extremes. Sci. Adv., 6, eaaz4571, https://doi.org/10.1126/sciadv.aaz4571, 2020

https://doi.org/10.5194/egusphere-2025-5893
Preprint. Discussion started: 4 December 2025

802 Chen, D. T., Huang, F. R., Li, Q., Li, L. H.: Spatial variation of humidity and its influencing factors in the
803 north and south slopes of the Tianshan Mountains, China during 1966-2015, Adv. Clim. Chang. Res., 14,
804 562, doi:10.12006/j.issn.1673-1719.2018.061, 2018.
805 Chen, L.: Changes and Their Impact Factors of Wind Speed (Energy) Over China under the Background
806 of Climate Warming (Doctoral dissertation). Nanjing University of Information Science and Technology,
807 2013.
808 Chen, W., Wang, L., Feng, J., Wen, Z., Ma, T., Yang, X., and Wang, C.: Recent progress in studies of the
809 variabilities and mechanisms of the East Asian monsoon in a changing climate. Advances in
810 Atmospheric Sciences, 36(9), 887-901, 2019.
811 Chen, Y., Liao, Z., Shi, Y., Tian, Y., and Zhai, P.: Detectable increases in sequential flood-heatwave
812 events across China during 1961–2018. Geophysical Research Letters, 48(6), e2021GL092549, 2021.
813 Chen, Z. F., Wang, L., Li, X. H., et al.: Spatiotemporal Change Characteristics of Extreme Precipitation
814 in South western China and its Relationship with Intense ENSO Events. Plateau Meteorology, 41(3):
815 604-616. doi: 10.7522/j.issn.1000-0534.2022.00004, 2022.
816 Ding, Y. H., Li, X., Li, Q. P.. Advances of surface wind speed changes over China under global
817 warming. J. Appl. Meteor. Sci., 31(1): 1-12. doi: 10.11898/1001-7313.20200101, 2020.
818 Ding, Y. H., Si, D., Liu, Y. J., et al.: On the characteristics, driving forces and inter-decadal variability of
819 the East Asian summer monsoon. Chinese Journal of Atmospheric Sciences (in Chinese), 42(3), 533-558,
820 doi:10.3878/j.issn.1006-9895．1712．17261, 2018.
821 Ding, Y., Li, Y.: A review on climatology of Afro-Asian summer monsoon and its long-term variability,
822 Journal of Tropical Meteorology, 32(6), 786-796, 2016.
823 Federal Emergency Management Agency: Multi-hazard loss estimation methodology: Hurricane model
824 Hazus®–MH MR5, Tech. Manual, Dep. of Homeland Security Federal Emergency Manage, Agency
825 Mitigation Div., Washington, D. C., 2013.
826 Guo, H., Xu, M., Hu, Q.: Changes in near-surface wind speed in China: 1969–2005, International Journal
827 of Climatology, 31(3), 349-358, doi:10.1002/joc.2091, 2011.
828 Hamid, S. S., Pinelli, J. P., Chen, S. C., and Gurley, K. J. N. H. R.: Catastrophe model-based assessment
829 of hurricane risk and estimates of potential insured losses for the state of Florida, Natural Hazards
830 Review, 12(4), 171–176, 2011.

https://doi.org/10.5194/egusphere-2025-5893
Preprint. Discussion started: 4 December 2025

831 Jiang, D. B., Tian, Z. P.: East Asian monsoon change for the 21st century: Results of CMIP3 and CMIP5
832 models. Chin. Sci. Bull., 58, doi: 10.1007/s11434-012-5533-0, 2013.
833 Jones, P. D., and Hulme, M.: Calculating regional climatic time series for temperature and precipitation:
834 methods and illustrations, Int. J. Climatol., 16, 361-377,
835 doi:10.1002/(SICI)1097-0088(199604)16:4<361::AID-JOC 53>3.0.CO;2-F, 1996.
836 Knutson, T., Camargo, S. J., Chan, J. C. L., Emanuel, K., Ho, C. H., Kossin, J., et al.: Tropical cyclones
837 and climate change assessment: Part II: Projected response to anthropogenic warming, Bulletin of the
838 American Meteorological Society, 101(3), E303–E322, doi:10.1175/BAMS-D-18-0194.1, 2020.
839 Liberato, M. L.: The 19 January 2013 windstorm over the North Atlantic: large-scale dynamics and
840 impacts on Iberia, Weather and Climate Extremes, 5, 16-28, 2014.
841 Li, D., Chen, Y., Messmer, M., Zhu, Y., Feng, J., Yin, B., and Bevacqua, E.: Compound wind and
842 precipitation extremes across the Indo-Pacific: Climatology, variability, and drivers, Geophysical
843 Research Letters, 49(14), e2022GL098594, 2022.
844 Li, Q., S. Yang, W. Xu, X. L. Wang, P. Jones, D. Parker, L. Zhou, Y. Feng, and Gao, Y.: China
845 experiencing the recent warming hiatus, Geophys. Res. Lett., 42, 889-898, doi:10.1002/2014GL062773,
846 2015.
847 Liu, M. H., Ren, H. L., Zhang, W. J., Ren, P. F.: Influence of super El Ni(n)o events on the frequency of
848 spring and summer extreme precipitation over eastern China, Acta Meteorologica Sinica, 76(4), 539-553,
849 doi:10.11676/qxxb2018.021, 2018.
850 Liu, Y., Cai, W., Sun, C., Song, H., Cobb, K. M., Li, J., et al.: Anthropogenic aerosols cause recent
851 pronounced weakening of Asian Summer Monsoon relative to last four centuries, Geophysical Research
852 Letters, 46(10), 5469-5479, 2019.
853 Lui, Y. S., Tam, C. Y., and Lau, N. C.: Future changes in Asian summer monsoon precipitation extremes
854 as inferred from 20-km AGCM simulations, Climate Dynamics, 52(3), 1443–1459,
855 doi:10.1007/s00382-018-4206-3, 2019.
856 Mann, H. B.: Nonparametric tests against trend, Econometrica, 13, 245–259, doi:10.2307/1907187,
857 1945.
858 Martius, O., Pfahl, S., and Chevalier, C.: A global quantification of compound precipitation and wind
859 extremes, Geophys. Res. Lett., 43, 7709–7717, doi:10.1002/2016GL070017, 2016.

https://doi.org/10.5194/egusphere-2025-5893
Preprint. Discussion started: 4 December 2025

Ma, X., Gao, X., Liu, Y.: Simulations of Aerosol Influences on the East Asian Winter Monsoon, Journal of applied meteorological science, 29(3), 333-343, 2018.

Miao, C. S., Song, P., Wang, J. H., et al.: Comparative Study of Impact Factors of the Yellow River Cyclones over the Bohai Sea in Spring and Summer, Meteorological Monthly, 41, 1068-1078, doi: 10.7519/j.issn.1000-0526.2015.08.003, 2015.

Naumann, G., and Coauthors: Global changes in drought conditions under different levels of warming, Geophys. Res. Lett., 45, 3285–3296, doi:10.1002/2017GL076521, 2018.

Pu, Y. L., Hong, Q., Feng, J.: Influence of developing phase of El Nino events on summer extreme precipitations in eastern China, Journal of Beijing Normal University (Natural Science), 60, 242-249, doi:10.12202/j.0476-0301.2023035, 2024.

Raveh-Rubin, S. and Wernli, H.: Large-scale wind and precipitation extremes in the Mediterranean: A climatological analysis for 1979–2012, Q. J. R. Meteorol. Soc., 141, 2404–2417, doi:10.1002/qj.2531, 2015.

Raymond, C., R. Horton, J. Zscheischler, O. Martius, A. AghaKouchak, J. Balch, S. Bowen, S. Camargo, J. Hess, K. Kornhuber, M. Oppenheimer, A. Ruane, T. Wahl, and White, K.: Understanding and managing connected extreme events, Nat. Clim. Change, 10, 611-621, doi:10.1038/s41558-020-0790-4, 2020.

Ridder, N. N., Ukkola, A. M., Pitman, A. J., and Perkins-Kirkpatrick, S. E.: Increased occurrence of high impact compound events under climate change, Npj Climate and Atmospheric Science, 5(1), 1–8, doi:10.1038/s41612-021-00224-4, 2022.

Ridder, N. N., Pitman, A. J., Westra, S., Ukkola, A., Do, H. X., Bador, M., et al.: Global hotspots for the occurrence of compound events, Nature Communications, 11(1), 5956, doi:10.1038/s41467-020-19639-3, 2020.

Rodgers, E. B., Chang, S. W., and Pierce, H. F.: A satellite observational and numerical study of precipitation characteristics in western North-Atlantic tropical cyclones, J. Appl. Meteorol., 33, 129–139, doi:10.1175/1520-0450(1994)033<0129:Asoans>2.0.Co;2, 1994.

Seneviratne, S. I., et al.: Changes in climate extremes and their impacts on the natural physical environment, in Managing the Risks of Extreme Events and Disasters to Advance Climate Change Adaptation, A Special Report of Working Groups I and II of the Intergovernmental Panel on Climate

https://doi.org/10.5194/egusphere-2025-5893
Preprint. Discussion started: 4 December 2025

Change (IPCC), edited by C. B. Field et al., pp. 109–230, Cambridge Univ. Press, U. K., and New York, 2012.

Sen, P. K.: Estimates of the regression coefficient based on Kendall's tau, J. Am. Stat. Assoc., 63, 1379-1389, doi:10.1080/01621459.1968.10480934, 1968.

Shi, J., Wen, K., and Cui, L.: Patterns and trends of high impact weather in China during 1959–2014, Nat. Hazards Earth Syst. Sci., 16, 855–869, doi:10.5194/nhess-16-855-2016, 2016.

Shi, X. H., Xu, X. D.: Interdecadal change of East Asian winter monsoon and a numerical experiment on its possible cause, J. Appl. Meteor. Sci., 18(6): 776-782, 2007.

Sun, Y., Ding, Y. H.: Responses of South and East Asian summer monsoons to different land-sea temperature increases under a warming scenario, Chinese Sci Bull, 56, doi: 10.1007/s11434-011-4602-0, 2011.

Sussman, H. S., Raghavendra, A., Roundy, P. E., and Dai, A.: Trends in northern midlatitude atmospheric wave power from 1950 to 2099, Climate Dynamics, 54(5–6), 2903–2918, 2020.

Stocker, B. D., and Coauthors: Multiple greenhouse-gas feed backs from the land biosphere under future climate change scenarios, Nat. Climate Change, 3, 666–672, doi:10.1038/nclimate1864, 2013.

Theil, H.: A rank-invariant method of linear and polynomial regression analysis. In Henri Theil's contributions to economics and econometrics: Econometric theory and methodology, Dordrecht: Springer Netherlands, 345-381, 1992.

Tilloy, A., Malamud, B. D., and Joly-Laugel, A.: A methodology for the spatiotemporal identification of compound hazards: Wind and precipitation extremes in Great Britain (1979–2019), Earth System Dynamics, 13(2), 993-1020, 2022.

Trenberth, K. E., Dai, A., vanderSchrier, G., Jones, P. D., Barichivich, J., Briffa, K. R., and Sheffield, J.: Global warming and changes in drought, Nat. Climate Change, 4, 17–22, doi:10.1038/nclimate2067, 2014.

Van den Hurk, B., van Meijgaard, E., de Valk, P., van Heeringen, K. J., and Gooijer, J.: Analysis of a compounding surge and precipitation event in the Netherlands, Environmental Research Letters, 10(3), 035001, 2015.

Waliser, D., and Guan, B.: Extreme winds and precipitation during landfall of atmospheric rivers, Nature Geoscience, 10(3), 179–U183, 2017.

https://doi.org/10.5194/egusphere-2025-5893
Preprint. Discussion started: 4 December 2025

Wang, R., Lü, G., Ning, L., Yuan, L., and Li, L.: Likelihood of compound dry and hot extremes increased with stronger dependence during warm seasons, Atmos. Res., 260, 105692, doi:10.1016/j.atmosres.2021.105692, 2021.

Wang, X. L., Feng, Y., Compo, G. P., Swail, V. R., Zwiers, F. W., Allan, R. J., and Sardeshmukh, P. D.: Trends and low frequency variability of extra-tropical cyclone activity in the ensemble of twentieth century reanalysis, Climate Dynamics, 40(11), 2775–2800, doi:10.1007/s00382-012-1450-9, 2013.

Wang, Y. N., Du, J., Mao, R.: Impact of large-scale climate factors on flood disasters in China in the past 40 years, Journal of Beijing Normal University (Natural Science), 57(6), 825-833, doi:10.12202/j.0476-0301.2021008, 2021.

Wan, H., Zhong, Z., Yang, X., et al.: Impact of city belt in Yangtze River Delta in China on a precipitation process in summer: a case study, Atmospheric Research, 125(3), 63-75, doi:10.1016/j.atmosres.2013.02.004, 2013.

Wu, W. B., You, Q. L., Wang, D.: Characteristics of Extreme Precipitation in China Based on Homogenized Precipitation Data, Journal of Natural Resources, 31(6), 1015-1026, doi:10.11849/zrzyxb.20150209, 2016.

Wu, G. X., Li, Z. Q., Fu, C. B., Zhang, X. Y., Zhang, R. Y., Zhang, R. H., Zhou, T. J., Li, J. P., Li, J. D., Zhou, D. G., Wu, L., Zhou, L. T., He, B., Huang, R. H.: Advances in studying interactions between aerosols and monsoon in China, Science China: Earth Sciences, doi: 10.1007/s11430-015-5198-z, 2015.

Xiong, Y., Xin, X., Kou, X.: Simulation and Projection of Near-Surface Wind Speeds in China by BCC-CSM Models, J. Meteorol. Res., 33(1), 149–158, doi:10.1007/s13351-019-8043-z, 2019.

Xu, X., Du, Y., Tang, J., and Wang, Y.: Variations of temperature and precipitation extremes in recent two decades over China, Atmos. Res., 101, 143-154, doi:10.1016/j.atmosres.2011.02.003, 2011.

Yaddanapudi, R., Mishra, A., Huang, W., and Chowdhary, H.: Compound wind and precipitation extremes in global coastal regions under climate change, Geophysical Research Letters, 49(15), e2022GL098974, doi:10.1029/2022GL098974, 2022.

Yamaguchi, M., Chan, J. C. L., Moon, I. J., Yoshida, K., and Mizuta, R.: Global warming changes tropical cyclone translation speed, Nature Communications, 11(1), 47, doi:10.1038/s41467-019-13902-y, 2020.

Yu, R., and Zhai, P.: More frequent and widespread persistent compound drought and heat event observed in China, Sci. Rep., 10, 14576, doi:10.1038/s41598-020-71312-3, 2020.

https://doi.org/10.5194/egusphere-2025-5893
Preprint. Discussion started: 4 December 2025

948 Zhang, Y., Chen, F. H., Gou, X. H., et al.: The temporal and spatial distribution of seasonal dry-wet
949 changes over the northwestern China: Based on PDSI, Acta Geographica Sinica, 62, 1142,
950 doi:10.3321/j.issn:0375-5444.2007.11.003, 2007.
951 Zhang, Y., Sun, X., Chen, C.: Characteristics of concurrent precipitation and wind speed extremes in
952 China, Weather and Climate Extremes, 32, 100322, 2021.
953 Zhou, B. Y., Zheng, F., and Zhu, J.: Analysis of the interannual variations and influencing factors of
954 wind speed anomalies over the Beijing–Tianjin–Hebei region, Atmospheric and Oceanic Science
955 Letters, 10(4), 312-318, doi:10.1080/16742834.2017.1327301, 2017.
956 Zhu, R., and Chen, L.: Climatic characteristics of the Jianghuai cyclone and its linkage with precipitation
957 during the Meiyu period from 1961 to 2020, Nat. Hazards Earth Syst. Sci., 24, 1937-1950,
958 doi:10.5194/nhess-24-1937-2024, 2024.
959 Zscheischler, J., and Seneviratne, S. I.: Dependence of drivers affects risks associated with compound
960 events, Sci. Adv., 3, e1700263, doi:10.1126/sciadv.1700263, 2017.
961 Zscheischler, J., Naveau, P., Martius, O., Engelke, S., and Raible, C. C.: Evaluating the dependence
962 structure of compound precipitation and wind speed extremes, Earth system dynamics, 12(1), 1-16,
963 2021.
964 Zscheischler, J., Martius, O., Westra, S., Bevacqua, E., Raymond, C., Horton, R. M., Hurk, B. V. D.,
965 AghaKouchak, A., Jézéquel, A., Mahecha, M. D., Maraun, D., Ramos, A. M., Ridder, N. N., Thiery, W.,
966 and Vignotto, E.: A typology of compound weather and climate events, Nat. Rev. Earth. Env., 1, 333-347,
967 doi:10.1038/s43017-020-0060-z, 2020.